Appl. Phys. A 56, 185–192 (1993)

Applied Physics A Solids and Surfaces

The Growth of Crystalline Vapor Deposited Carbon-60 Thin Films

W. Krakow*, N. M. Rivera, R. A. Roy, R. S. Ruoff, J. J. Cuomo

IBM Research Division, T. J. Watson Research Center, Yorktown Heights, NY 10598, USA

Received 14 October 1992/Accepted 7 December 1992

Abstract. Thin films (25–2500 Å) of C_{60} molecules have been deposited on both (001) NaCl and mica substrates at varying temperatures by resistive evaporation. Both electron diffraction and high resolution microscopy have been used to assess the degree of crystallinity, the orientational ordering and the nature of the defects present in these face-centered-cubic films. For NaCl, optimum conditions yielded polycrystalline films with a tendency towards a ⟨110⟩ orientation, while for mica, extended single crystal films have been fabricated which exhibit a ⟨111⟩ direction normal to the film surface.

PACS: 61.10, 68.55

In recent years, the fabrication in large quantities of fullerenes, C_{60} and related caged molecules has made possible studies of the structural properties of this form of carbon in the crystalline state [1–3]. One of the earliest studies of well-formed three-dimensional solvent-free bulk crystals up to 0.4 mm diameter used C_{60} material heated in a quartz tube which was allowed to condense in a cooler region [4]. Single-crystal X-ray diffraction at room temperature shows that the molecules are centered at the sites of a face-centered-cubic (fcc) Bravais lattice ($a_0 = 14.2$ Å), with a high degree of rotational disorder. High-resolution synchrotron X-ray powder diffraction was used more recently to study solid C_{60} between 11 and 300 K [5]. It was found that a low-temperature phase exists below 249 K with diffraction peaks that can be indexed as simple-cubic reflections with mixed odd and even indices and were referred to as forbidden fcc reflections. The unit cell consisted of four molecules as in the fcc case but it has undergone a phase transition where the C_{60} units which were arranged equivalently become inequivalent. Somewhat earlier in time, a study of a mixture of C_{60}/C_{70} bulk material using electron diffraction and high-resolution microscopy has revealed a hexagonal close packed phase which quickly degraded under the electron beam [6]. It was not noted that the reflections could be classified as being of the mixed type. Because of the appreciable solvent concentrations, these reflections could be caused by localized defects which produce void-like regions and hence local regions of simple cubic structure rather than a hexagonal structure.

Several thin-film studies have been undertaken to understand the earliest stages of C_{60} growth. It is reasonable to expect that highly ordered C_{60} thin films will have superior properties for certain applications such as superconductivity. Single and multilayer growths of C_{60} on (110) GaAs at 300 K and elevated temperatures have been studied by scanning tunneling microscopy [7]. For these van der Waals solids, both equilibrium and nonequilibrium structures were found with a lack of preference of binding sites on the substrate, except where large corrugations or substrate steps exist. A similar study in the monolayer growth regime of sublimed C_{60} on mica substrates was performed by helium atom scattering [8]. This work demonstrated that a single monolayer of C_{60} grew epitaxially at room temperature with a periodicity of 10.4 Å, which is approximately double that of the unit cell dimension perpendicular to the (001) mica basal plane (5.2 Å). For thicker films, a preliminary investigation of C_{60} deposited on MoS_2 substrates was reported to produce 0.1 μm thick films measuring 1.5 cm × 1.5 cm. Electron diffraction was used and it was claimed that the films were defect free and monocrystalline [9].

Along similar lines to the above thin film studies, we concurrently have grown thin films of C_{60} molecules on both (100) NaCl and (001) mica and characterized the films' crystallinity and local structural arrangements of the C_{60} molecules. Here we present the results of our vapor deposition experiments.

1 Experimental Procedures

1.1 Specimen Preparation

Commercially prepared carbon soot was extracted with toluene and the resulting C_{60} was chromatographically sep-

* *Present address:* Mountainside Trail, Peekskill, NY 10566, USA (Fax: +1-914/737-4023

arated, as reported in prior literature [2, 3]. Mass spectrometry of the powder indicated that no oxygen was bound to the molecules. Films were then prepared by loading pristine C_{60} into an alumina coated tungsten crucible which could be resistively heated in a vacuum evaporation chamber. The chamber was evacuated by a dry pump which reached a base pressure in the 10^{-5} Torr range during deposition. The crucible was heated to maintain a deposition rate of about 0.25 Å/s, as measured by a quartz crystal oscillator calibrated for the deposition geometry used. The chamber pressure remained constant during the deposition, indicating that no volatile solvents were present in the C_{60} powder. The temperature of both types of substrates (NaCl and mica) were varied in a series of depositions from unheated (RT) to 100, 150, 200, 250° C, by use of a quartz radiant heater placed in back of the substrate holding plate. One of the substrates employed was 0.75 in × 0.75 in muscovite mica sheets, $KAl_3Si_3O_{10}(OH)_2$, which was double cleaved to provide clean surfaces on both sides of the sample prior to loading in the deposition system. The second type of sample, (001) NaCl, was air cleaved and water polished to remove any cleavage steps prior to the deposition. Most films were grown to a thickness of 150 Å except at 200° C, where both 500 Å and 2500 Å films were also grown. Additional thin films were grown at RT from 25 Å on up in thickness to assess whether individual cage units could be observed.

1.2 Electron Microscopy

For electron microscopy, the thin films of C_{60} were removed from the NaCl and mica by lift-off onto the surface of water. The films were then mounted on 300 or 1000 mesh gold microscope grids. The microscopy was performed with a JEOL 4000EX microscope operating at 400 kV incident beam energy. The point resolution of this microscope is better than 1.7 Å in the axial illumination mode. Bright-field images with magnifications up to 300,000 × were recorded with great care to avoid any noticeable beam damage. Images taken with a minimum dose were unaffected by the electron beam. It was only after prolonged exposure that damage became apparent.

2 Results and Discussion

2.1 Films Deposited onto (100) NaCl

For deposits onto NaCl and substrate temperature below 100° C, the C_{60} films were amorphous-like in appearance. In the very thin deposits of ≈25 Å at RT there appear to be some features which could correspond to fullerene cage structures as displayed in Fig. 1. However, these results are inconclusive since the film is, on average, three C_{60} units thick. The projection of overlapping structures would cause considerable confusion even though the microscope is performing to the 1.7 Å resolution level.

An example of a 150 Å thick C_{60} deposited at a 100° C substrate temperature is given in Fig. 2. Here, there is evidence of the onset of crystallization since small ordered patches of lattice can be discerned (see arrows). The coarse granular structure observed here is analogous to the finer structure observed in arc evaporated carbon films. This implies that the film consists of C_{60} molecules arranged in an almost amorphous-like state.

Increasing the NaCl substrate temperature to 150° C produced polycrystalline films as evidenced by the micrographs of Fig. 3. Here Fig. 3a is at a lower magnification that shows relatively large connected crystalline patches by diffraction contrast. Although the film is free standing there still remains an appreciable amount of voids. This observation indicates that the film growth was more three-dimensional than layer-by-layer. The higher magnification view in Fig. 3b shows the crystalline nature of this film. Two strong orientations can be observed by measuring the lattice plane spacings and their corresponding intersection angles. On the left portion of the micrograph is a region which is in the (111) orientation since three sets of {220} type lattice planes are present measuring ≈5.0 Å. In the middle and right portions are (110) orientations since orthogonal sets of lattice planes of 7.1 Å corresponding to the {200} type reflections and the 5.0 Å {220} type are present. This latter result shows that a preferred orientation with a common ⟨110⟩ zone axis normal to the film plane is present as was confirmed by electron diffraction and will be presented shortly as part of Fig. 5. It should be noted for these (110) orientations that a large number of planar defects such as twins and stacking faults can be observed. Here both $\Sigma = 3$ tilt boundaries are present as well as a number of stacking faults occuring on {111} planes.

At 200° C substrate temperature, two examples of films deposited on NaCl are displayed in Fig. 4 for a 150 Å thickness in Fig. 4a and a 500 Å thickness in Fig. 4b. In Fig. 4a large plate-like, faceted crystallites are present some of which appear edge-on while others appear inclined. It is believed that this film collapsed such that many of the platelets which were once in a single plane have now become inclined during the lift-off process. The platelets were very loosely connected which permitted the buckling to occur when the film was removed from the NaCl substrate. For a thicker film shown in Fig. 4b, the platelets have grown together and only a few holes remain in the film. It is also apparent that some planar defects are present. Similar features are also present at 250° C substrate temperature. However, at this elevated temperature the C_{60} molecules do not adhere to the substrate as well and extended deposition times are required. At 300° C, C_{60} films cannot be grown since the material reevaporates from the surface faster than the deposition rate.

The behavior of C_{60} growth on NaCl is summarized by the diffraction patterns displayed in Fig. 5 which shows the progression from 100 to 250° C in 50 Å increments. At 100° C the film has an amorphous-like structure with nanocrystallites. The larger spacings at the center of the pattern show that the nearest neighbor spacings of ≈8.7 Å are present. At 150° C, the film is polycrystalline and there is a tendency towards a (110) preferred orientation owing to the dominant {111} type Bragg reflections present. At the higher temperature of 200 and 250° C, the films are more randomly oriented as evidenced by the strong {200} rings. In no case was strong epitaxy found for the (100) NaCl substrate. A possible future direction would be to prepare other NaCl orientations such as (110), (111) as examples to evaluate whether single crystal films could be grown.

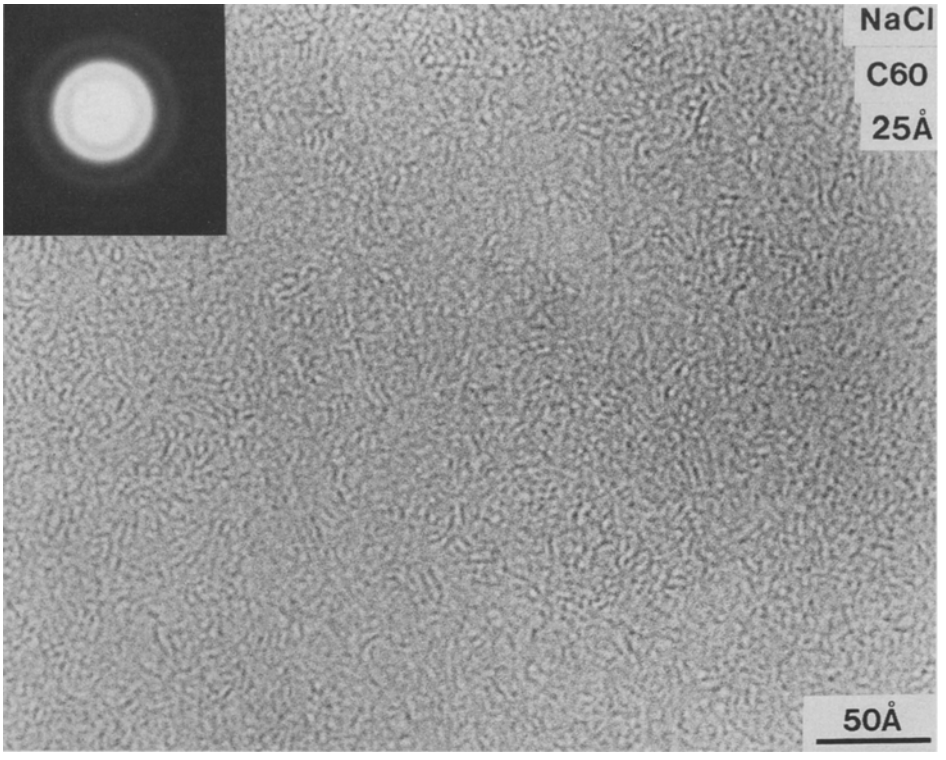

Fig. 1. Bright-field micrograph of a 25 Å thick C_{60} film deposited at room temperature on (100) NaCl. Original microscope magnification 600,000 ×

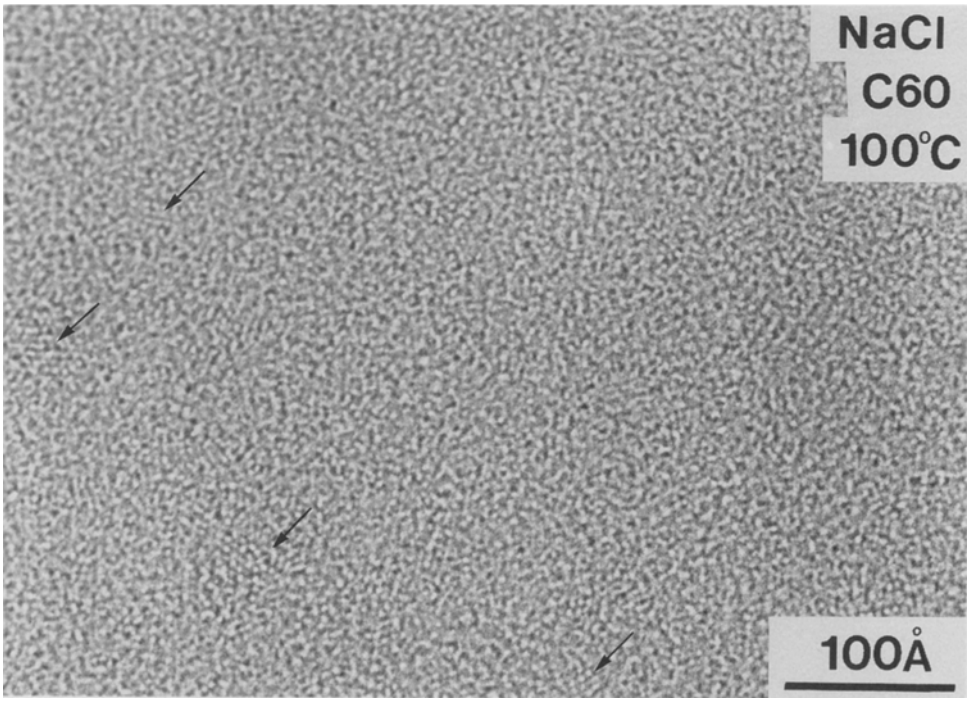

Fig. 2. Bright-field micrograph of a 150 Å C_{60} film deposited on NaCl at 100° C. Original magnification 300,000 ×

2.2 Films Deposited onto Mica

For deposits onto mica the same temperature conditions were used as the NaCl depositions. Often substrates of both types were placed in the vacuum chamber side by side which then permitted direct comparisons. At the lower temperatures of 100° C or less there was no discernable difference between the deposits on NaCl and NaCl which appeared amorphous-like in the micrographs. However, for a 150° C substrate temperature a noticable difference occurred in which case the films on mica exhibited well oriented crystallographic features. Figure 6 is an example of a 150 Å deposited film where at the lower magnification in Fig. 6a the crystalline regions appear darker due to their strong diffraction contrast. The edges of the crystalline regions appear to follow the three possible ⟨110⟩ trace directions which are rotated by 120° with respect to each other. These features are characteristic of (111) fcc crystallites. This is directly confirmed by

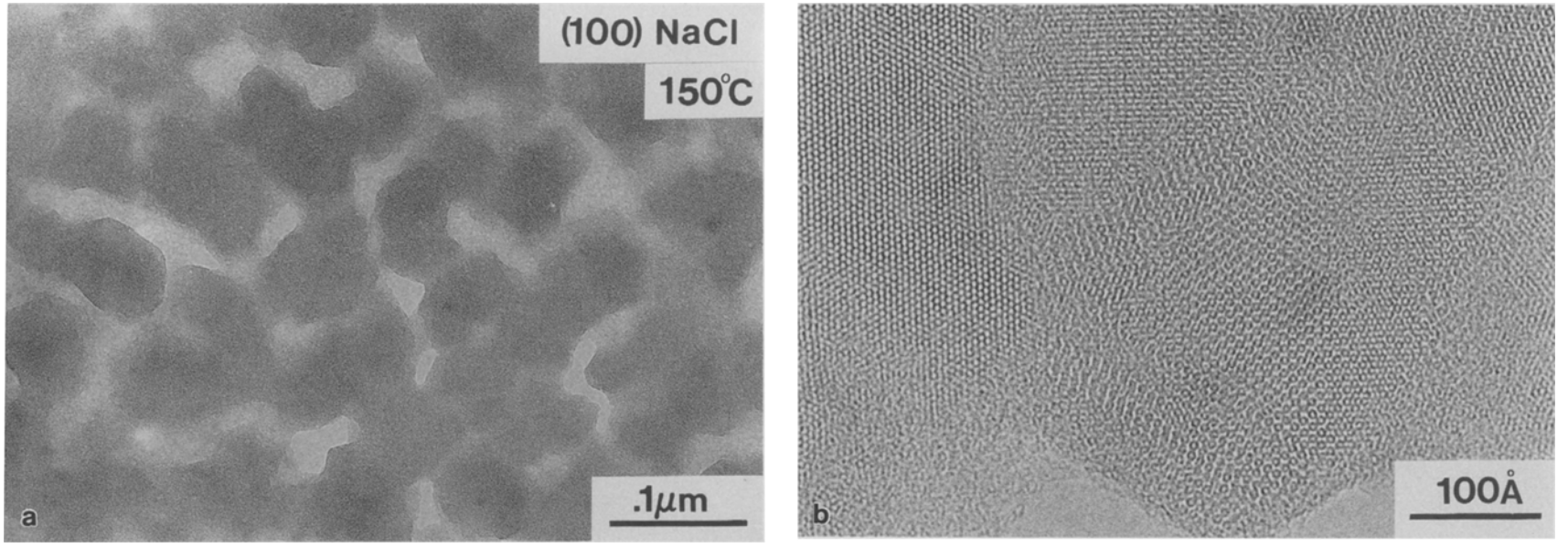

Fig. 3a, b. Bright-field micrographs of C_{60} films deposited onto (100) NaCl at 150° C. **a** Low magnification, **b** high magnification

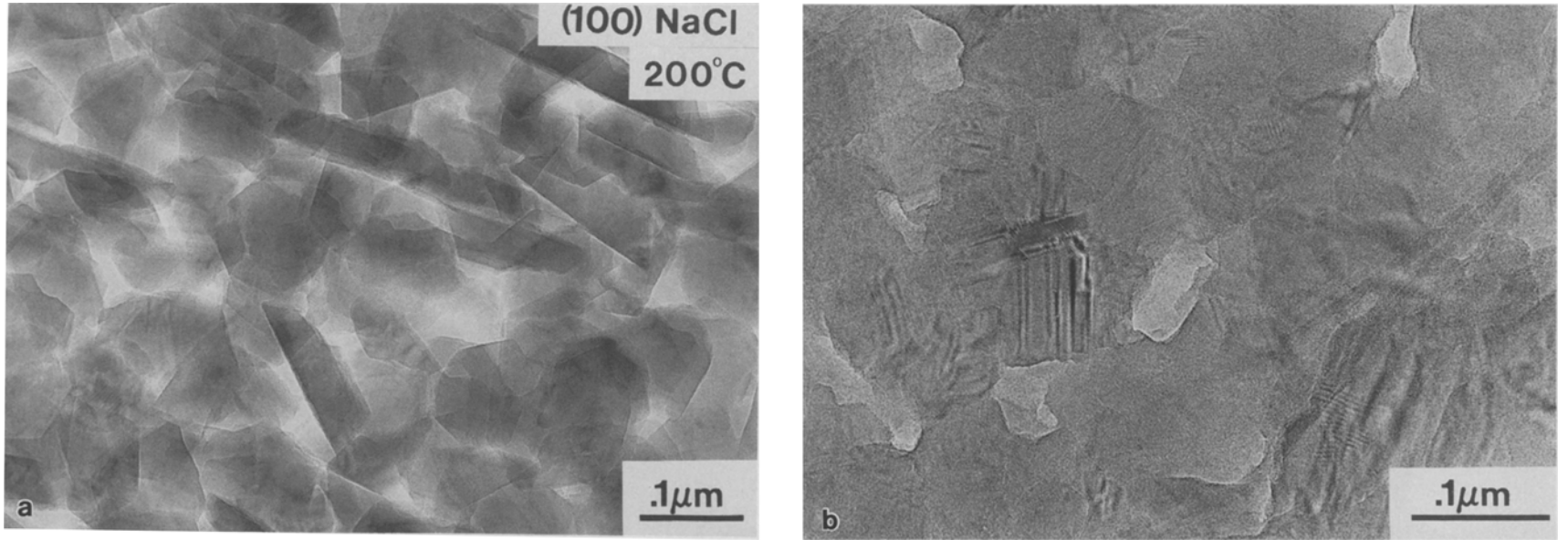

Fig. 4a, b. Low magnification bright-field micrographs of C_{60} deposited on (100) NaCl at 200° C. **a** 150 Å thickness, **b** 500 Å thickness

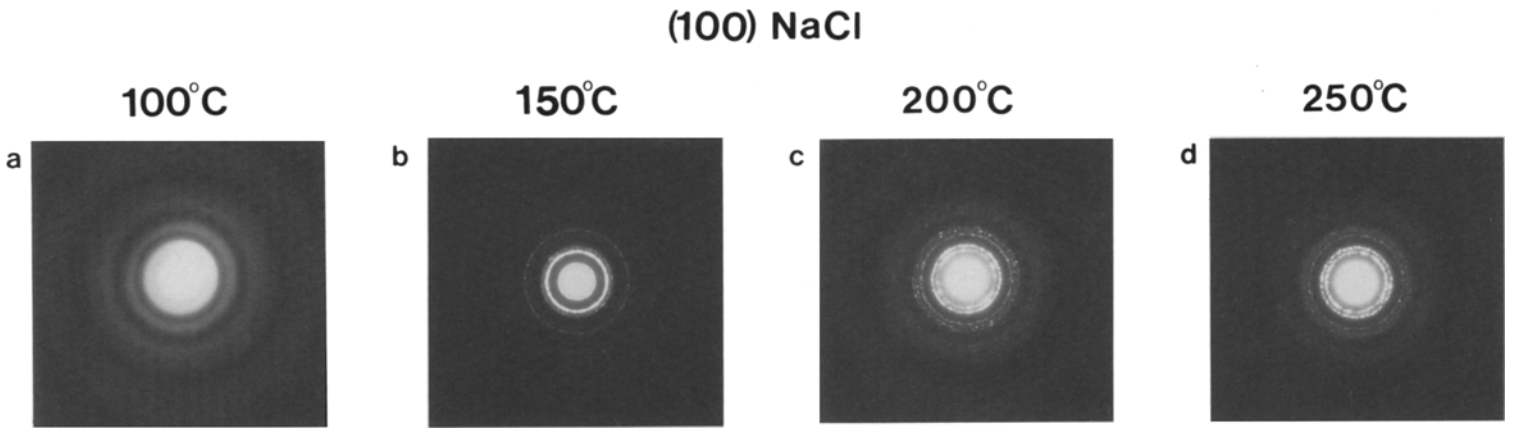

Fig. 5a–d. Selected area diffraction patterns of C_{60} films 150 Å thick deposited on NaCl at different temperatures. **a** 100° C, **b** 150° C, **c** 200° C, **d** 250° C

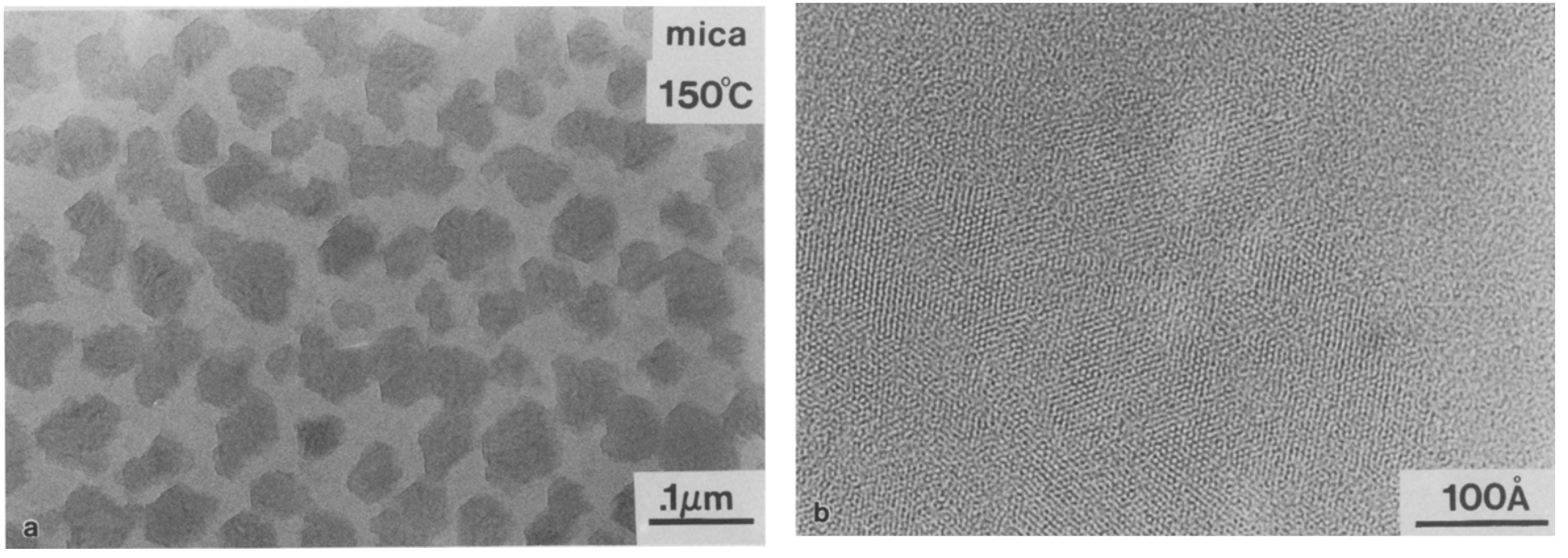

Fig. 6a, b. Low magnification **a**, and high magnification bright-field images of C_{60} deposited on mica at 150° C. Original magnifications, **a** 40,000 ×, **b** 300,000 ×

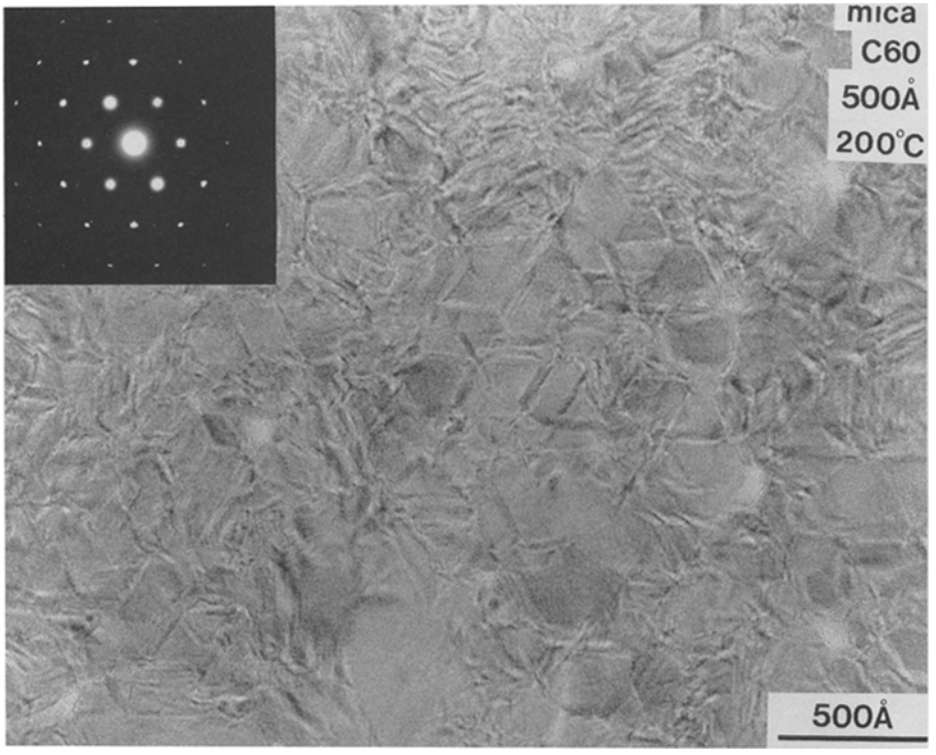

Fig. 7. Low magnification bright-field micrograph of a 500 Å C_{60} film deposited on mica at 200° C

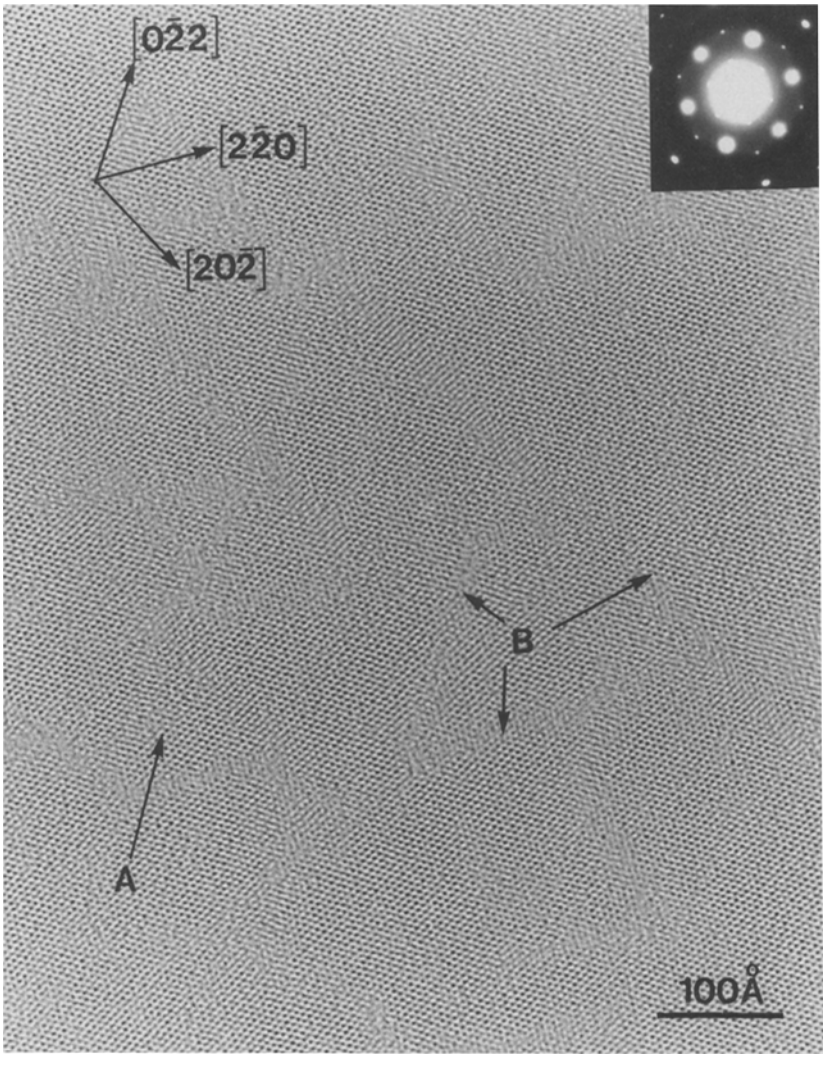

Fig. 8. High-resolution bright-field image of a (111) C_{60} thin film deposited at 200° C. The direction indicated by the letter A shows the monolayer lattice of ≈ 8.7 Å periodicity. Regions marked B show planar defects. Original microscope magnification 300,000 ×

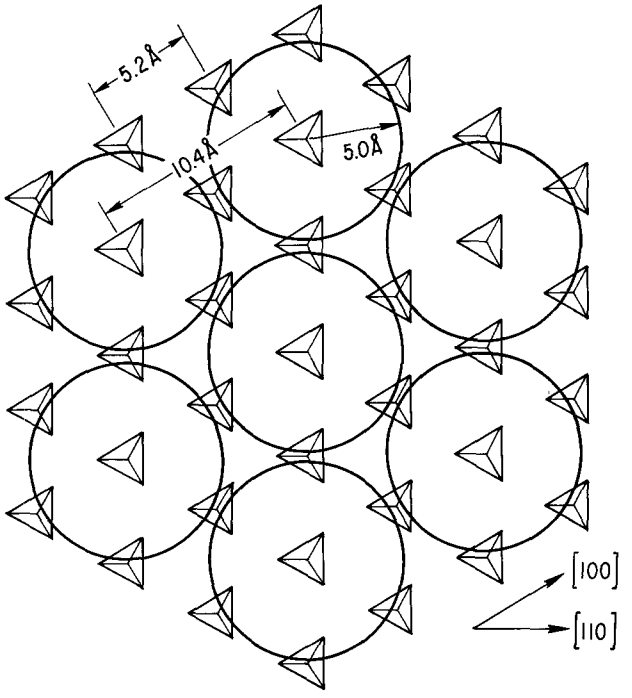

Fig. 9. Schematic view of mica hexagonal SiO_4 tetrahedron layer and a C_{60} monolayer. Here a silicon atom is located at the center of each tetrahedron and an oxygen at each corner. C_{60} molecules are depicted as large heavy circles

inspecting the lattice planes in the higher magnification view shown in Fig. 6b which has bulk lattice spacings corresponding to $\{220\}$ type reflections ($d = 5.0$ Å). The region between the crystallite in Fig. 6a, b is amorphous-like. The right-hand side of the high magnification image (Fig. 6b) shows the characteristic random granular appearance observed in disordered material.

For a substrate temperature of 200° C, high quality, single crystal C_{60} films were obtained as demonstrated by the low magnification bright-field image and diffraction pattern insert of Fig. 7 for a 500 Å thick film. The strong first-order bulk lattice reflections of the diffraction pattern insert are of the $\{220\}$ type which is expected for molecules arranged in a fcc film with a [111] normal to the film surface. The next strong spacings are of the $\{422\}$ type ($d = 2.9$ Å). These results are very similar to earlier investigations where metal films were epitaxially deposited on mica at moderate substrate temperatures [10]. Inspection of Fig. 7 also reveals that there are contrast variations which tend to follow $\langle 110 \rangle$ directions and are of finite width. These types of defects are planar and have also been observed in metals and can be classified as either double positioning boundaries (DPB) or stacking faults (SF). The DPB arise because different regions of the thin films are stacked as ABC layers while other regions are stacked in a reverse CBA sequence. Here every third plane of the film is continuous across a boundary. The boundary separating these two types of regions usually occurs on $\{111\}$ planes inclined to the film plane which are at angles of 70.5° C to the (111) surface. In the case of stacking faults, the boundary is also inclined on a $\{111\}$ plane with one part of the crystal being translated with respect to the other by a lattice translation vector of the type $\pm 1/3\langle 111 \rangle$. Furthermore, these types of defects produce little effect on the diffraction pattern since they arise through simple lattice translations.

For thinner C_{60} films of 150 A thickness grown at 200° C, a number of features are observed which cannot be seen in thicker films. Figure 8 shows a high-resolution bright-field micrograph of a single-crystal film and its diffraction pattern (insert). The diffraction pattern shows the strong first-order $\{220\}$ bulk lattice reflections of 5.0 Å. The faint innermost reflections, with corresponding spacings of 8.7 Å, appear much sharper than the bulk lattice spots and cannot

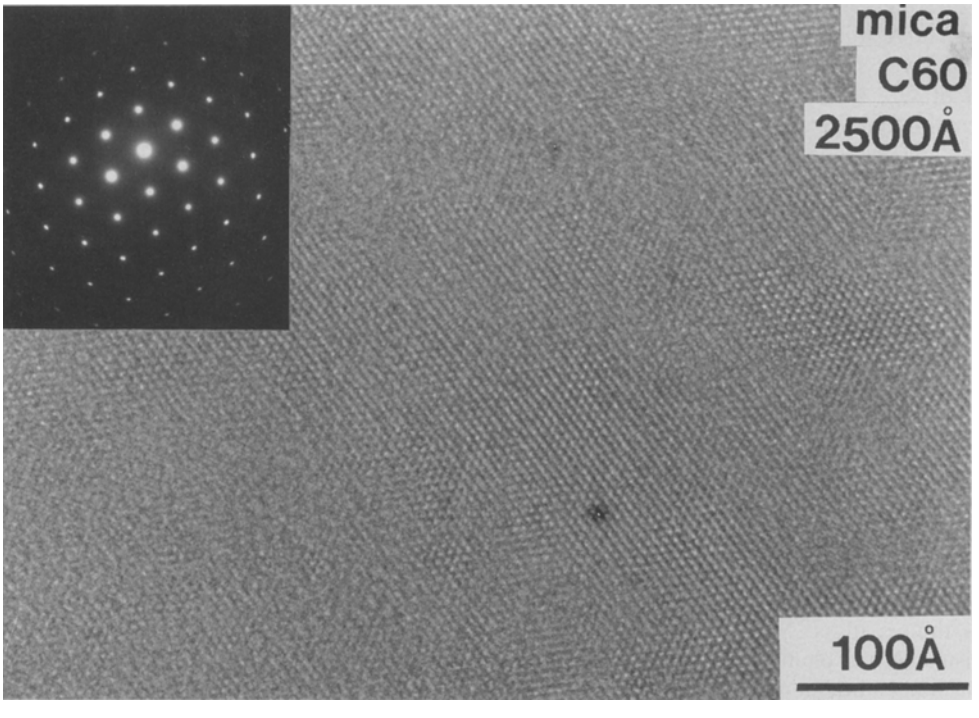

Fig. 10. Bright-field image of a (111) 2500 Å thick C_{60} film grown on mica. Original magnification 300,000 ×

be indexed in the fcc system since they would then have mixed indices. These faint spots occur at the 1/3{422} locations which is characteristic of forbidden reflections due to incomplete layer stacking seen in prior studies of fcc metal systems grown in (111) orientations [11, 12]. Also evidenced in the thicker film diffraction pattern of Fig. 7, much weaker 1/3{422} reflections are present since the relative diffraction intensity due to incomplete stacking is diminished. These reflections should not be confused with a hexagonal lattice, and are present only because excess monolayers occur due to incomplete stacking of bulk layers. These layers, while part of the whole film, individually form a hexagonal two-dimensional net with planar spacings of ≈ 8.7 Å.

Returning to the bright-field image of the 150 Å thick C_{60} film deposited on mica shown in Fig. 8, three sets of lattice fringes are present which are arranged in a hexagonal mesh indicative of the diffent {220} type reflections. The lattice fringe contrast was adjusted by changing the microscope objective lens focus to produce black spot images where C_{60} molecules are located. Because the image is a phase contrast image, it lacks the high contrast typically found in diffraction contrast imaging. However, careful inspection of the images reveals that the monolayer corrugation periodicities are present when there is incomplete layer stacking. These can be seen by examining the micrograph almost edge-on and viewing along the faint fringe directions. As an example, one direction has been labeled by an arrow marked A along one of the three possible directions which are rotated by 60° from strong bulk lattice fringe directions. It should be noted that these fringes are not necessarily continuous owing to the fact that different regions may have different termination layers, i.e. A or B or C. If an integral number of layers is present totaling $3N$, no termination fringes will be visible. Also, we cannot discern whether the excess termination is on the top or bottom surface. This latter point has been explained for thin (111) Au films [11]. The same rules apply to the thin fullerene films fabricated here. Since the planar spacings of (111) planes is ≈ 8.2 Å, the total number of layers of fullerenes which form a 150 Å thick (111) film is approximately 18. The repeat in layer sequence ABC is 3×8.2 Å; hence, each column of C_{60} units visualized in Fig. 8, i.e. each black dot, contains an average of six molecules. It is therefore plausible that a change of one C_{60} unit in a column occupancy would produce a small but visible contrast effect.

Further examination of Fig. 8 also reveals that additional contrast variations are present which tend to follow $< 110 >$ directions and are of finite width, as indicated by several of the regions marked by the letter B. As previously mentioned, these contrast variations are produced by either double positioning boundaries or stacking faults. Stacking errors occur in the crystal when these types of boundaries are encountered and a washing out of lattice fringes occurs which is just perceptible in the regions labeled B. In other words, the fullerene columns are not aligned in projection above and below the planar defect. For thicker films, the defects appear wider and hence cause the lattice images to be more complicated. However, it is believed that the surface topography is similar to that of the thinner films.

Next, the question of lattice mismatch and planar defect origin can be addressed. Here, the (111) oriented single-crystal thin films of C_{60} have been deposited on muscovite mica and the cleavage plane of the mica is defined by the potassium layer sandwiched between two hexagonal sheets of SiO_4 tetrahedra [13]. The in-plane periodicity of these hexagonal arrays is 5.2 Å. A view of a hexagonal layer of tetrahedron units is shown in Fig. 9. Here C_{60} units of 10.04 Å diameter are indicated by large circles that have been superimposed to show a likely geometrical correspondence to the mica. It can be seen that the mica can act as a template on a local scale since the mismatch between the mica and C_{60} radius unit spacings is about 3.4%. This mismatch can readily account for the occurrence of planar defects over a distance of a few hundred angstroms or less. A lattice translation produced by a planar defect for the C_{60} lattice would maintain the proper coincidence with the underlying mica template.

Finally, an example of a 2500 Å C_{60} film deposited on mica at 200° C is shown in Fig. 10. While the lattice fringes are somewhat degraded and dynamical diffraction effects are present, the single-crystal structure is clear and the orientation corresponds to (111) as was present in the thinner films. The purpose here is to show that continuous, single-crystal films may be grown over extended dimensions of the mica substrates as large as 0.75 in × 0.75 in. Using a favorable evaporation geometry, it is expected that the dimensions could be extended to several inches on a side.

In summary, we have observed that the onset of crystallinity in C_{60} films deposited by evaporation occurs between 100 and 150° C. The substrate plays a crucial role in determining the degree of epitaxy, with films deposited on mica showing a single crystal structure. The growth of epitaxial films over a wide range of film thickness on inexpensive substrates provides the basis for better fundamental property measurements as well as improved properties for C_{60}-derived materials.

References

1. H.W. Kroto, J.R. Heath, S.C. O'Brien, R.F. Curl, R.E. Smalley: Nature **318**, 162 (1985)
2. W. Krätschmer, K. Fostiropoulos, D.R. Huffman: Chem. Phys. Lett. **170**, 167 (1990)
3. W. Krätschmer, L.B. Lamb, K. Fostiropoulos, D.R. Huffman: Nature **347**, 354 (1990)
4. R.M. Fleming, T. Siegrist, P.M. Marsh, B. Hessen, A.R. Kortan, D.W. Murphy, R.C. Haddon, R. Tycko, G. Dabbagh, S.M. Mujsce, M.L. Kaplan, S.M. Zuhurak: Mat. Res. Soc. Symp. Proc. **206**, 691 (1991)
5. P.A. Heiney, J.E. Fischer, A.R. McGhie, W.J. Romanow, A.M. Denenstein, J.P. McCauley Jr., A.B. Smith, III: Phys. Rev. Lett. **66**, 2911 (1991)
6. G. van Tendeloo, M. Op DeBeeck, S. Amelinckx, J. Bohr, W. Krätschmer: Europhys. Lett. **15** 295 (1991)
7. Y.Z. Li, J.C. Patrin, M. Chander, J.H. Weaver, L.P.F. Chibante, R.E. Smalley: Science **252**, 547 (1991) and **253**, 429 (1991)
8. D. Schmicker, S. Schmidt, J.G. Skofronickk, J.P. Toennies, R. Vollmer: Phys. Rev. B **44**, 10995 (1991)
9. M. Sakurai, H. Tada, K. Saiki, A. Koma: Jpn. J. Appl. Phys. **2**; Lett. **30**, 11a, L1892 (1991)
10. D.W. Pashley: Phil. Mag. **4**, 316 (1959)
11. W. Krakow: Thin Solid Films **93**, 235 (1982)
12. D. Cherns: Phil. Mag. **30**, 549 (1974)
13. R. Elandsson, G. Hadziioannou, C. M. Mate, G. M. McClelland, S. Chaing: J. Chem. Phys. **89**, 5190 (1988)